Quantifying uncertainties in soil carbon responses to changes in global mean temperature and precipitation

K. Nishina, A. Ito, D. Beerling, P. Cadule, Philippe Ciais, D. Clark, P. Falloon, A. Friend, R. Kahana, E. Kato, et al.

Earth Syst. Dynam., 5, 197–209, 2014
www.earth-syst-dynam.net/5/197/2014/
doi:10.5194/esd-5-197-2014

Earth System Dynamics
Open Access

Quantifying uncertainties in soil carbon responses to changes in global mean temperature and precipitation

K. Nishina[1], A. Ito[1], D. J. Beerling[6], P. Cadule[7], P. Ciais[7], D. B. Clark[4], P. Falloon[3], A. D. Friend[5], R. Kahana[3], E. Kato[1], R. Keribin[5], W. Lucht[2], M. Lomas[6], T. T. Rademacher[5], R. Pavlick[8], S. Schaphoff[2], N. Vuichard[7], L. Warszawaski[2], and T. Yokohata[1]

[1]National Institute for Environmental Studies, 16-2, Onogawa, Tsukuba, Ibaraki, Japan
[2]Potsdam Institute for Climate Impact Research, Telegraphenberg A 31, 14473 Potsdam, Germany
[3]Met Office Hadley Centre, FitzRoy Road, Exeter, Devon, EX1 3PB, UK
[4]Centre for Ecology and Hydrology, Wallingford, OX10 8BB, UK
[5]Department of Geography, University of Cambridge, Downing Place, Cambridge, CB2 3EN, UK
[6]Department of Animal and Plant Sciences, University of Sheffield, Sheffield, S10 2TN, UK
[7]Laboratoire des Sciences du Climat et de l'Environment, Joint Unit of CEA-CNRS-UVSQ, Gif-sur-Yvette, France
[8]Max Planck Institute for Biogeochemistry, Hans-Knöll-Str. 10, 07745 Jena, Germany

Correspondence to: K. Nishina (kazuya.nishina@gmail.com)

Received: 27 August 2013 – Published in Earth Syst. Dynam. Discuss.: 12 September 2013
Revised: 19 January 2014 – Accepted: 21 February 2014 – Published: 2 April 2014

Abstract. Soil organic carbon (SOC) is the largest carbon pool in terrestrial ecosystems and may play a key role in biospheric feedbacks with elevated atmospheric carbon dioxide (CO_2) in a warmer future world. We examined the simulation results of seven terrestrial biome models when forced with climate projections from four representative-concentration-pathways (RCPs)-based atmospheric concentration scenarios. The goal was to specify calculated uncertainty in global SOC stock projections from global and regional perspectives and give insight to the improvement of SOC-relevant processes in biome models. SOC stocks among the biome models varied from 1090 to 2650 Pg C even in historical periods (ca. 2000). In a higher forcing scenario (i.e., RCP8.5), inconsistent estimates of impact on the total SOC (2099–2000) were obtained from different biome model simulations, ranging from a net sink of 347 Pg C to a net source of 122 Pg C. In all models, the increasing atmospheric CO_2 concentration in the RCP8.5 scenario considerably contributed to carbon accumulation in SOC. However, magnitudes varied from 93 to 264 Pg C by the end of the 21st century across biome models. Using the time-series data of total global SOC simulated by each biome model, we analyzed the sensitivity of the global SOC stock to global mean temperature and global precipitation anomalies (ΔT and ΔP respectively) in each biome model using a state-space model. This analysis suggests that ΔT explained global SOC stock changes in most models with a resolution of 1–2 °C, and the magnitude of global SOC decomposition from a 2 °C rise ranged from almost 0 to 3.53 Pg C yr^{-1} among the biome models. However, ΔP had a negligible impact on change in the global SOC changes. Spatial heterogeneity was evident and inconsistent among the biome models, especially in boreal to arctic regions. Our study reveals considerable climate uncertainty in SOC decomposition responses to climate and CO_2 change among biome models. Further research is required to improve our ability to estimate biospheric feedbacks through both SOC-relevant and vegetation-relevant processes.

1 Introduction

Soil organic carbon (SOC) is considered to be the largest carbon pool in terrestrial ecosystems (Davidson and Janssens, 2006). Soil provides many ecosystem services, such as regulating, provisioning, and societal services (Breure et al., 2012). In ecosystem services, SOC is critical for ensuring sustainable food production owing to its nutrient retention function and water-holding capacity (Lal, 2004, 2010). Thus,

the maintenance of SOC is important for global and social sustainability (e.g., Mol and Keesstra, 2012). In climate systems, because of the vast carbon pool of SOC, the behavior of SOC is key for understanding the feedback of terrestrial ecosystems to atmospheric CO_2 concentrations in a warmer world (Heimann and Reichstein, 2008; Thum et al., 2011). However, a large number of uncertainties exist in the observation and modeling of SOC dynamics (e.g., Post et al., 1982; Todd-Brown et al., 2013). For example, in the Coupled Model Intercomparison Project Phase 5 (CMIP5), Todd-Brown et al. (2013) reported that the (simulated) present-day global SOC stocks range from 514 to 3046 Pg C among 11 Earth system models (ESMs). Soil processes in terrestrial ecosystem models are significantly simpler than actual processes or above-ground processes, and thus exist structural uncertainties in SOC dynamics in ESMs.

Temperature and precipitation are critical factors for the feedback of terrestrial ecosystems to atmospheric CO_2 (Seneviratne et al., 2006). Similarly, SOC dynamics are strongly affected by temperature and precipitation, because SOC dynamics in biome models are parameterized as a function of soil temperature, moisture, and other factors (e.g., Davidson and Janssens, 2006; Ise and Moorcroft, 2006; Falloon et al., 2011). The differences in these functions and their parameters have important effects on the projection of global SOC stocks and their behavior (Davidson and Janssens, 2006; Ise and Moorcroft, 2006).

In this study, we examined the SOC dynamics simulated by seven biome models as part of the Inter-Sectoral Impact Model Intercomparison Project (ISI-MIP) (Warszawski et al., 2014), which were forced using the bias-corrected outputs of five global climate models (GCMs) in newly developed climate scenarios, i.e., representative concentration pathways (RCPs). We aimed to investigate the impact of climate change on the global SOC stock with respect to changes in global mean temperature and precipitation and explore the uncertainties in future global SOC stock projections.

In order to analyze the first-order behavior of the simulated global SOC-dynamics, we focused on the interannual responses of the biome models under the assumption that SOC is one-compartment of Earth's system. First, we considered global SOC dynamics as the following simple, differential equation:

$$\frac{\mathrm{dSOC}}{\mathrm{d}t} = \mathrm{Input} - k\,\mathrm{SOC}, \quad (1)$$

where Input is carbon derived primarily from photosynthesis products via chemical and microbial humification (Wershaw, 1993), and k is the global SOC turnover rate. In most conventional models (Li et al., 2014), SOC decomposition functions as a first-order decay process as in Eq. (1). SOC dynamics are regulated by the balance between the input from vegetation biomass carbon and SOC decomposition. In this study, we examined a simple hypothesis: can global mean temperature and precipitation anomalies (ΔT (°C) and ΔP (%), respectively) be used as explanatory variables of global SOC decomposition dynamics in future (projections over the 21st century). If true, this would mean that ΔT and ΔP can explain k during a projection period in biome models. This simplification enables us to review the global impact of climate change on SOC dynamics and identify the characteristics of biome models especially in global SOC behavior. Subsequently, we assessed whether the time evolution of the estimation uncertainties for SOC can be explained by ΔT and ΔP sensitivities during the 21st century for each biome model. Furthermore, we compared the spatial distributions of global SOC pools and their changes to evaluate regional differences, focusing on detailed processes in the interaction with vegetation dynamics.

2 Materials and methods

2.1 Method and models

In this study, we examined SOC processes using seven biome models obtained from the ISI-MIP. The biome models are Hybrid4 (Friend and White, 2000), JeDi (Jena Diversity-Dynamic Global Vegetation model) (Pavlick et al., 2013), JULES (Joint UK Land Environment Simulator; Clark et al., 2011; Best et al., 2011), LPJmL (Lund–Potsdam–Jena managed land Sitch et al., 2003), SDGVM (Sheffield Dynamic Global Vegetation Model; Woodward et al., 1995), VISIT (Vegetation Integrative Simulator for Trace gases) (Ito and Oikawa, 2002; Ito and Inatomi, 2012), and ORCHIDEE (Organizing Carbon and Hydrology in Dynamic Ecosystems; Krinner et al., 2005). In this study, Hybrid4, JeDi, JULES, and LPJmL are dynamic global vegetation models, and the others are fixed vegetation models, in this study. General information about SOC processes is summarized in Table 1.

In the ISI-MIP framework, these models were run with 5 GCM × 4 RCP scenarios and a fixed CO_2 control was also run with RCP8.5 climate condition scenarios. In this study, for the biome model forcing, we used climate variables in HadGEM2-ES (HadGEM – Hadley Centre Global Environmental Model) with bias correction for temperature and precipitation from Hempel et al. (2013). For the spin-up of each model, we used de-trending forcing data for the years 1951–1980 repeatedly until reaching equilibrium of VegC (vegetation carbon) and SOC. For CO_2, we used the CO_2 concentration for 1950 while running the 30 yr spin-ups. The global climate variables (atmospheric CO_2 concentration, global mean terrestrial temperature anomaly ΔT (°C), and global terrestrial precipitation anomaly ΔP (%)) in each RCP scenario for HadGEM are summarized in Fig. 1. ΔT and ΔP were set to 0 as the averages of their values between 1980 and 2000. In addition, there was no anthropogenic land-use change for the entire simulation period in this study. More detail about the experimental setup is available in the literature (Warszawski et al., 2014).

Table 1. Description of SOC-relevant processes in each biome model.

Model	$f(T)$*	$f(M)$*	Compartment	Permafrost	Soil depth	Citation
Hybrid4	Exponential with optimum	Optimum curve	8	None	Non-explicit	Friend and White (2000)
JeDi	Exponential (Q_{10}; 1.4)	none	1	None	Over 5 m	Pavlick et al. (2013)
JULES	Exponential (Q_{10}; 2.0)	Linear with plateau	4	None	Non-explicit	Clark et al. (2011)
LPJmL	Lloyd & Taylor	Linear	2	Considered	3 m	Sitch et al. (2003)
SDGVM	Optimum curve	Optimum curve	4	None	1 m	Woodward et al. (1995)
VISIT	Lloyd & Taylor	Optimum curve	1	None	1 m	Ito and Inatomi (2012)
ORCHIDEE	Exponential (Q_{10}; 2.0)	Quadratic	3	None	Non-explicit	Krinner et al. (2005)

* $f(T)$ and $f(M)$ indicate the function of temperature and moisture sensitivities of SOC. Compartments indicates the number of SOC compartment considered in SOC pool (e.g., slow, fast decomposition compartments included in LPJmL).

2.2 Estimation of ΔT and ΔP sensitivity of global SOC

We used a state-space model (more properly vector autoregression) (Sims and Zha, 1998) to evaluate the sensitivity of global SOC decomposition to global temperature and precipitation anomalies in each biome model. This vector autoregression model considers only process uncertainty, not observation uncertainty in a state-space model. We applied this analysis to annual global SOC time-series data in each biome model simulated in the five scenarios (three scenarios for ORCHIDEE), i.e., the four RCPs and the fixed CO_2 experiment with RCP8.5 climate conditions in HadGEM (Figs. 1, 2).

We first modeled the likelihood function using the following equation. The model outputs were archived for each year; therefore, we discretized the equation as the annual time step t.

$$\mathrm{SOC}_{[n,t]} \sim \text{normal}\left(\mu_{[n,t-1]},\ \sigma_{\mathrm{ps}}\right), \tag{2}$$

where $\mathrm{SOC}_{[n,t]}$ is the global SOC stock at time t (year) in scenario n, and σ_{ps} is the process error. $\mu_{[n,t-1]}$ is defined as follows:

$$\mu_{[n,t-1]} = \alpha\,\mathrm{VegC}_{[n,t-1]} + e^{\left(-k-\beta_1\Delta T_{[n,t-1]}-\beta_2\Delta P_{[n,t-1]}\right)}\,\mathrm{SOC}_{[n,t-1]}, \tag{3}$$

where $\mathrm{VegC}_{[n,t]}$ indicates the global vegetation biomass C stock at time t in scenario n, and α is the fraction of VegC transformed into SOC per year, which is assumed to represent the annual input of SOC. k is the turnover rate for global SOC (yr^{-1}) under standardized global mean temperature and precipitation conditions (averages between 1980 and 2000). β_1 and β_2 are the global SOC sensitivities to ΔT and ΔP, respectively (units: $\mathrm{yr}^{-1}\,\Delta T^{-1}$ and $\mathrm{yr}^{-1}\,\Delta P^{-1}$).

The priors of these parameters are defined as follows:

$$\sigma_{\mathrm{ps}} \sim \text{uniform}\,(0,\ 100), \tag{4}$$
$$\alpha \sim \text{uniform}\,(0,\ 0.1), \tag{5}$$
$$k \sim \text{uniform}\,(0,\ 1), \tag{6}$$
$$\beta_1 \sim \text{normal}\,(0,\ 100), \tag{7}$$
$$\beta_2 \sim \text{normal}\,(0,\ 100). \tag{8}$$

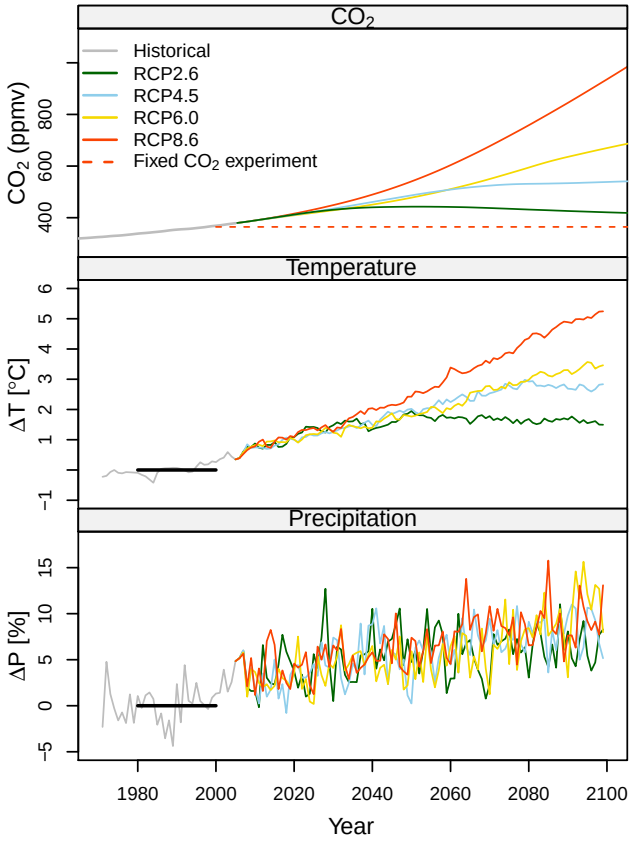

Fig. 1. Climate variables for CO_2 (RCPs), and global mean annual temperature and global annual precipitation anomalies in HadGEM.

We used vague priors for β_1 and β_2 to estimate the ΔT and ΔP effect on k. For α and k, we used uniform priors, which are sufficiently broad theoretically.

Then, the joint posterior is given by following equation.

$$p\left(\alpha,\ \beta_1,\ \beta_2,\ k,\ \sigma_{\mathrm{pr}}|\mathrm{data}\right) \sim p\left(\mathrm{data}|\alpha,\ \beta_1,\ \beta_2,\ k,\ \sigma_{\mathrm{pr}}\right) \times p(\alpha)\,p(k)\,p\left(\beta_1\right)\,p\left(\beta_2\right)\,p\left(\sigma_{\mathrm{pr}}\right). \tag{9}$$

We used the Hamiltonian Monte Carlo method to sample the posterior with STAN (Stan Development Team, 2012) and R (R Core Team, 2012).

2.3 Evaluation of stimulated global SOC decomposition in ΔT from posteriors

Using posteriors in the steady-state model, we simulated the global SOC decomposition stimulated by increased global mean temperature at $\Delta 2$, $\Delta 3$, and $\Delta 4\,^{\circ}$C.

$$\text{Stimulated SOC decomposition} = e^{(-k-\beta_1 \Delta T)}\,\text{SOC}_{2000} - e^{-k}\,\text{SOC}_{2000} \quad (10)$$

We used the global SOC stock SOC for the year of 2000 for each biome model to calculate the global SOC decomposition and obtained posterior simulations by drawing 1000 samples from the posterior distributions. From the 1000 iterations, we evaluated the predictive posterior intervals for the stimulated global SOC decomposition values at each ΔT.

In addition, to standardize the SOC_{2000} in each biome model, we used the value of 1255 Pg C (95 % CI; 891–1657 Pg C) estimated by Todd-Brown et al. (2013) instead of the original SOC_{2000} of each biome model to evaluate the effect of current SOC stocks on the global SOC decomposition to ΔT in each model. This procedure enable us to evaluate the effects of the estimated current global SOC stock in each model on the response to ΔT raising.

3 Results

3.1 Global SOC and VegC projection in HadGEM

The increase of ΔT depends on the RCP scenario, with the maximum increase in RCP8.5 being 7.5 °C in 2099 in HadGEM2. In RCP2.6, the maximum ΔT was 1.9 °C during the entire simulation period and showed signs of leveling off in 2050. In all RCP scenarios, ΔP increased to 11 (RCP4.5) and 16 % (RCP8.5). However, there were high amplitudes of ΔP within each RCP scenario; thus, there were no obvious differences between RCPs.

For 2000, in HadGEM, the global SOC stocks varied from 1090 (Hybrid4) to 2646 Pg C (JULES) between the biome models (Fig. 2). The mean global SOC stock in the six models was 1772 Pg C (standard deviation; 568 Pg C). An estimated empirical global SOC stock was 1255 Pg C (Todd-Brown et al., 2013). However, global VegC stocks in 2000 ranged from 510 (VISIT) to 1023 Pg C (JULES). The mean global VegC among the seven biome models was 809 Pg C (SD (standard deviation); 223 Pg C) (Fig. 2). The global VegC stocks in most models were comparable with the VegC (493 Pg C) estimated by the IPCC Tier-1 method (Ruesch and Gibbs, 2008).

In the projection period (2000–2099), the SOC stock in the six models (except for Hybrid4) increased in all RCPs compared to that in 2000. The global SOC stock in Hybrid4 continuously decreased in all RCPs during the projection period (Fig. 2). Under the RCPs, the maximum SOC stock increase for the projection period was observed in JeDi with RCP8.5, with a value of 347 Pg C. In the fixed CO_2 scenarios, the global SOC stocks continuously decreased in most biome models, showing global SOC changes from −299 to 65 Pg C at the end of the simulation period.

The global VegC stocks increased in nearly all RCPs and biome models compared to the global VegC in 2000. However, the global VegC stocks in Hybrid4 and LPJmL with RCP8.5 did not continuously increase in the projection period and were not the largest stock at the end of the simulation period during the projection period. In the fixed CO_2 scenarios, the global VegC stocks also continuously decreased, and global VegC changes ranged from −517 to −40 Pg C at the end of the simulation period (Fig. 2).

The rank order of the SOC stock over each RCP at the end of the simulation (2099) is in good agreement with the rank order of each corresponding VegC stock in the same period in JeDi, JULES, LPJmL, and SDGVM. However, the orders of the SOC stock in the other biome models are different than those of the global VegC stocks. These stock changes are attributed to the different SOC decomposition processes.

3.2 Posteriors of the state-space model; global SOC sensitivity to ΔT and ΔP

The Gelman and Rubin convergence statistics ($\hat{R}$) of all parameters were lower than 1.01 in all models; therefore, the parameters represented successful convergences (data not shown). The posterior distributions of the parameters for each biome model are summarized in Table 2.

α, which is the fraction of annual translation of VegC to SOC, among the biome models varied from 0.721 % in Hybrid4 to 3.860 % in VISIT. The SOC turnover rate k (yr^{-1}) ranged from 2.51×10^3 in LPJmL to $16.10 \times 10^3\,\text{yr}^{-1}$ in VISIT.

The 95 % credible intervals (CI) in sensitivity of global SOC to ΔT (β_1) in each biome model did not cover 0 in all models (Table 2). And the 95 % CI of β_1 in each model was not partially duplicated, which means that the sensitivity to ΔT could be statistically distinguished between the biome models. The highest β_1 was observed in VISIT, with a median value of $1.225 \times 10^{-3}\,\text{yr}^{-1}\,\Delta T^{-1}$ (or $^{\circ}\text{C}^{-1}$). The lowest β_1 was observed in JeDi and was approximately $0\,\text{yr}^{-1}\,\Delta T^{-1}$.

The sensitivity of global SOC to ΔP (β_2) in the biome models was lower compared to the SOC turnover rate k and β_1. Their values ($\text{yr}^{-1}\,\Delta P^{-1}$) were nearly one order of magnitude less than β_1. Considering the range of the values of ΔP in the projection period, the impact on global SOC stock dynamics is small in all biome models. Furthermore, the 95 % CIs of β_2 in each model were partially duplicated.

Table 2. Posteriors of statistical time-series analysis of each biome model.

Models	$\alpha \times 10^{-2}$ (fraction)	$k \times 10^{-3}$ (yr^{-1})	$\beta_1 \times 10^{-3}$ ($yr^{-1}\,\Delta T^{-1}$)	$\beta_2 \times 10^{-4}$ ($yr^{-1}\,\Delta P^{-1}$)	σ
Hybrid4	0.721 (0.663–0.781)	4.78 (4.35–5.23)	1.130 (0.885–1.039)	0.183 (−0.465–0.111)	0.932 (0.882–0.987)
JeDi	1.815 (1.762–1.867)	7.94 (7.86–8.21)	−0.058 (−0.041–−0.076)	0.001 (−0.006–0.008)	0.442 (0.419–0.467)
Jules	3.727 (3.430–4.033)	13.99 (12.81–15.20)	0.669 (0.613–0.723)	0.333 (0.158–0.504)	1.312 (1.242–1.384)
LPJmL	0.730 (0.687–0.771)	2.51 (2.34–2.68)	0.210 (0.190–0.231)	0.025 (−0.049–0.098)	0.522 (0.495–0.552)
SDGVM	1.820 (1.615–2.030)	6.50 (5.71–7.29)	0.333 (0.266–0.398)	0.365 (0.154–0.575)	0.936 (0.887–0.989)
VISIT	3.860 (3.761–3.958)	16.10 (15.68–16.53)	1.225 (1.181–1.257)	−0.121 (−0.119–−0.151)	0.371 (0.352–0.378)
ORCHIDEE*	1.343 (1.230–1.457)	7.01 (6.38–7.64)	0.903 (0.839–0.970)	−0.009 (−0.031–0.014)	1.001 (0.934–1.076)

* In ORCHIDEE, the parameters were estimated from time-series data compiled in three scenarios (RCP2.6, RCP8.5, and Fixed CO_2).

On the basis of the posterior parameters, we estimated the stimulated global SOC decomposition for Δ 2, Δ 3, and Δ 4 °C, assuming that each global SOC stock is at the 2000 level (Fig. 3). A statistical difference was observed among the Δ 2, Δ 3, and Δ 4 °C in five biome models (i.e., Hybrid4, JULES, LPJmL, VISIT, and ORCHIDEE). However, the magnitudes of the stimulated global SOC decomposition varied. At Δ 4 °C, it ranged from 1.9 (in LPJmL) to 8.1 Pg C yr^{-1} (in JULES). In SDGVM, there were no statistical differences in the stimulated global SOC decomposition between Δ 3 and Δ 4 °C. There were also no differences in this term among Δ 2, Δ 3, and Δ 4 °C in JeDi.

3.3 Latitudinal δSOC (2099–2000 and CO_2-fixed CO_2) in HadGEM RCP8.5

Latitudinal SOC stock in the HWSD (Figs. 4, 5a) displays a double peak in both the northern high latitudes and low latitudes. The most SOC stock is found around 60° N. In all biome models, large SOC stocks were also observed in high-latitude zones (50–75° N; Figs. 5a and S1 in the Supplement). However, the range of simulated SOC change during this century (kg C m^{-2}) in each biome model was different. The upper 99 percentile of SOC accumulation in each biome model varied from 23.8 in SDGVM to 97.6 kg C m^{-2} in LPJmL (Fig. S1 in the Supplement).

For differences between 2099 and 2000 in HadGEM RCP8.5, a large variance among biome models was observed between 30° S and 10° N (tropic region) and between 40 and 75° N (boreal to Arctic region) (Figs. 4, 5a) in the biome models. There were four types of latitudinal changes: (i) SOC increase in both regions (JeDi, SDGVM, ORCHIDEE), (ii) SOC increase in boreal to arctic regions and decrease in the tropics (JULES, VISIT), (iii) SOC increase in the tropics and decrease in boreal to arctic regions (LPJmL), and (iv) SOC decrease in both regions (Hybrid4). The maximum difference was observed in the boreal regions, where it reached more than 20 Pg $2.5°^{-1}$.

There were also differences between the increasing CO_2 scenario (RCP8.5) and the fixed CO_2 scenario with the RCP8.5 climate condition in SOC ($\Delta SOC_{CO_2-\text{fixed}\,CO_2}$) (Fig. 5c). This suggests that the increases of plant production and biomass due to CO_2 fertilizer effects in the increasing CO_2 scenario (RCP8.5) contributed to the SOC stock increases because of the increase of C input to soil (indirect CO_2 effect). We observed bimodal increases in six biome models, and the peaks were between 30 and 70° N and between 30° S and 10° N. In Hybrid4, the large SOC increase due to CO_2 was unimodal around the boreal regions. The maximum difference between the increasing CO_2 scenario and the fixed CO_2 scenario was observed around 60° N, which was approximately 10 Pg $2.5°^{-1}$

The different values of $\Delta SOC_{CO_2-\text{fixed}\,CO_2}/\Delta VegC_{CO_2-\text{fixed}\,CO_2}$ (Fig. 5d) indicate a different turnover rate of vegetation carbon to SOC (via litter) among the biome models and regions. This is because of the assumption of almost the same states except in VegC dynamics between RCP8.5 and fixed CO_2 scenarios. $\Delta SOC_{CO_2-\text{fixed}\,CO_2}/\Delta VegC_{CO_2-\text{fixed}\,CO_2}$ varied with latitude and among the biome models. In almost all the models, $\Delta SOC_{CO_2-\text{fixed}\,CO_2}/\Delta VegC_{CO_2-\text{fixed}\,CO_2}$ was the highest in the higher latitude regions. In the Hybrid4 model, the $\Delta SOC_{CO_2-\text{fixed}\,CO_2}/\Delta VegC_{CO_2-\text{fixed}\,CO_2}$ was relatively low in all regions, compared with other model results.

4 Discussion

4.1 Global mean temperature and precipitation impact(s) on global SOC decomposition and projection uncertainties

During the projection period (2000–2099), the global SOC stock changes in all RCPs (without the fixed CO_2 scenario) ranged from −6 to 280 Pg C under RCP2.6 (mean ± SD: 89 ± 104 Pg C). Under RCP8.5, the SOC changes varied from −124 to 392 Pg C (113 ± 176 Pg C) (Fig. 2) at the end of the projection period. These global SOC stock changes are equivalent to −185 to +58 ppmv in atmospheric CO_2 concentration. Thus, in higher radiative forcing scenarios, uncertainties associated with future global SOC projection increase. These ranges of the global SOC stock changes by 2099 were comparable with the VegC changes (Fig. 2). However, in the projection period, the global VegC stocks primarily act as sinks for atmospheric CO_2, while the global SOC

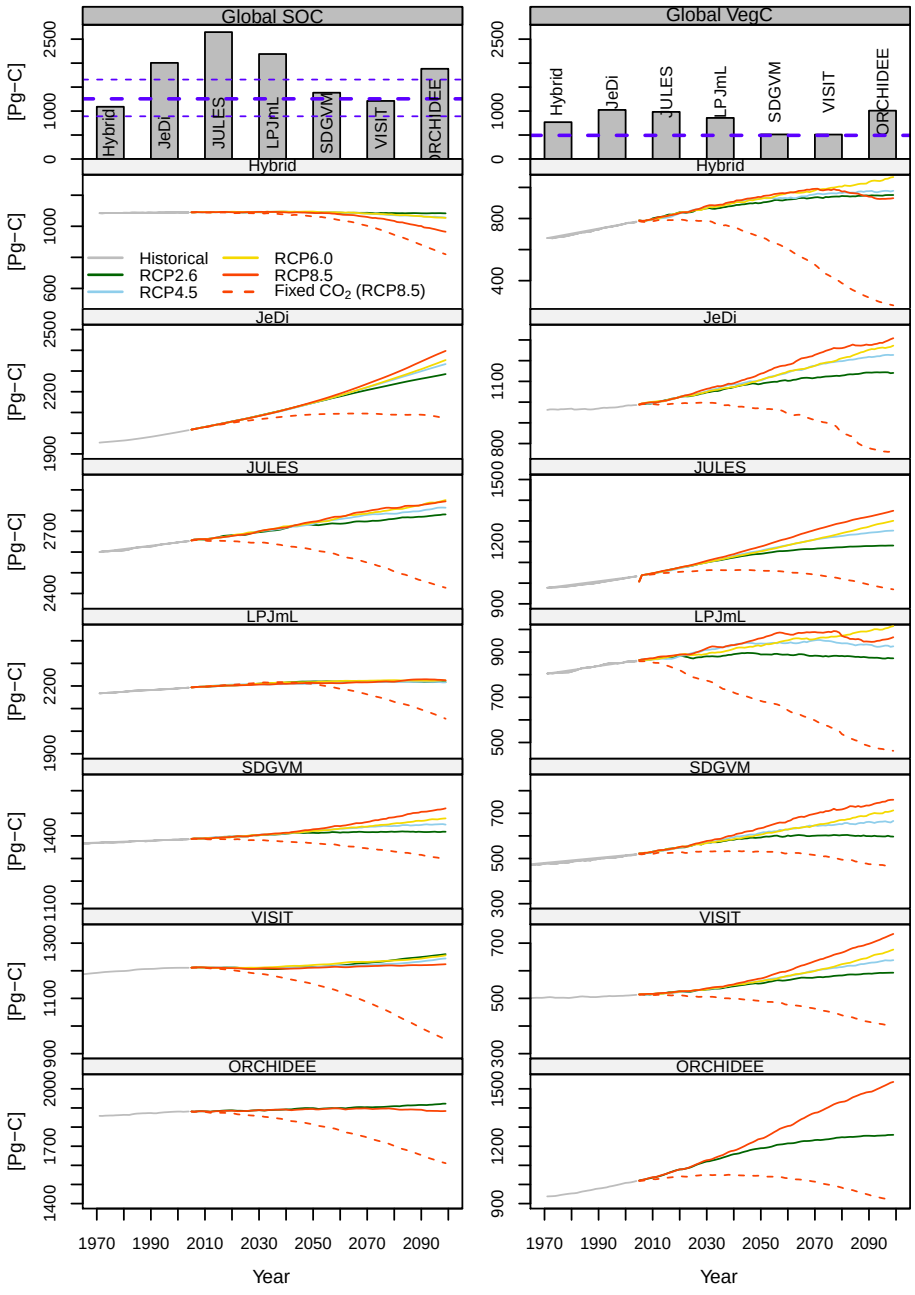

Fig. 2. Changes in global SOC and VegC stocks of each biome model in HadGEM forced by each RCP. Upper bar charts indicate global SOC and VegC stocks in 2000. In the bar chart for global SOC, blue lines indicate the empirical global SOC stock estimated by Todd-Brown et al. (2013) based on the Harmonized World Soil Database (solid line indicates mean and dotted lines indicate 95 % confidence intervals). In the bar chart for global VegC, blue lines indicates empirical global VegC stock estimated by Ruesch and Gibbs (2008).

stocks act as either sinks or sources depending on the biome model. There were similar SOC projections in the same period (2000–2100) from multiple model simulations in previous studies. In the C4MIP study, for example, the global SOC stock changes ranged from approximately −50 to 300 Pg by the end of the simulation period among the 11 coupled climate–carbon models (Friedlingstein et al., 2006; Eglin et al., 2010). It has also been predicted that SOC stocks in 2100 differ by approximately 200 Pg among five DGVMs under forced A1FI and B1 scenarios (Sitch et al., 2008), which is the highest forcing scenario in the AR4 assessment. Compared with these studies, the SOC changes simulated in this study varied comparably or showed slightly higher uncertainty than those of previous projections.

The magnitude of global SOC decomposition and the response to ΔT primarily depend on the amount of the

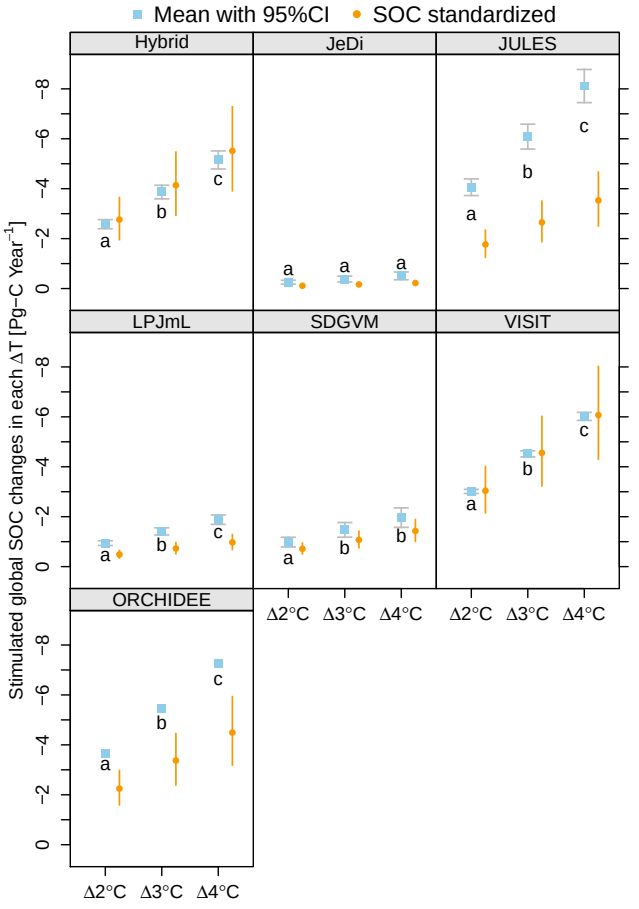

Fig. 3. Estimated global SOC changes in response to each ΔT in each biome model based on the original global SOC stock at 2000 (blue symbols) and standardized as the empirical global SOC stock (1255 Pg C, 95 % CI; 891–1657 Pg C) estimated in Todd-Brown et al. (2013). Different letters indicate no partial duplication among 95 % CI for each biome model (Table 2).

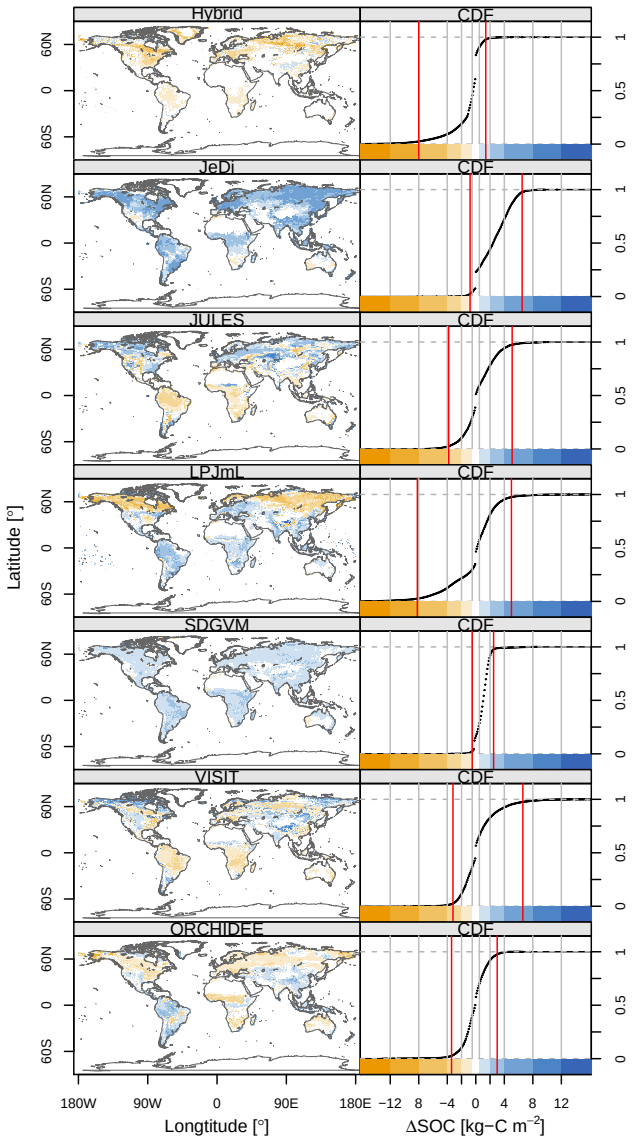

Fig. 4. Maps of SOC changes by 2099 from 2000 and cumulative density function (CDF) in each biome model in HadGEM RCP8.5. In the plot of CDF, red lines indicate 2.5 and 97.5 percentiles of SOC changes.

global SOC stock and a turnover rate of SOC decomposition process. As has been reported in a CMIP5 experiment (Todd-Brown et al., 2013), our study has also shown that simulated global present-day SOC stocks in seven ecosystem models show high variation (1090–2646 Pg C) compared to the variation of global present-day VegC stocks (Fig. 2). There were some estimations available for global SOC stock, ranging from 700 (Bolin, 1970) to 3000 Pg C (Bohn, 1976). The most widely cited studies (Post et al., 1982; Batjes, 1996) estimated global SOC stock to be about 1500 Pg C (0–100 cm depth). However, in the CMIP5 experiment, the simulated global SOC stock by ESMs varied from 510 to 3040 Pg C (Todd-Brown et al., 2013). Even though the global SOC stocks for the year 2000 in this study were within range of those in Todd-Brown et al. (2013), this SOC stock uncertainty could still invoke future projection uncertainty in SOC dynamics. To test this issue, we estimated the global SOC standardized impact of each ΔT by a simple substitution, which assumed that the global SOC stock in each biome model is equal to the value (1255 Pg C, 95 % CI; 891–1657 Pg C) empirically estimated from the new global data set by Todd-Brown et al. (2013). The standardized global SOC decomposition was smaller than the original SOC decomposition in some models, which showed large differences in the global SOC stocks compared to the reference SOC stock (Todd-Brown et al., 2013) (Figs. 2, 5). In addition, overall uncertainties among the biome models became relatively small by about 30 % in total variance. This shows that global SOC estimation is critical to the magnitude of SOC feedback. Thus, the estimated dynamic model revealed

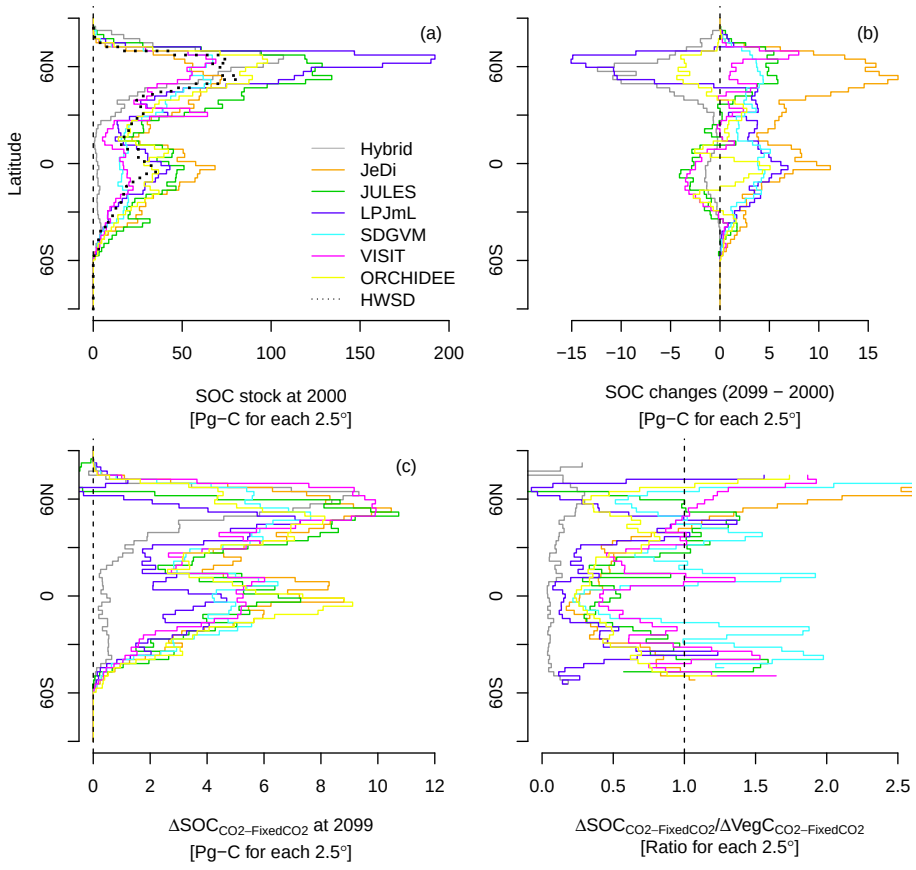

Fig. 5. Latitudinal SOC stocks **(a)**, SOC changes (2099–2000 in RCP8.5) **(b)**, and indirect CO_2 effect on SOC (CO_2 experiment–fixed CO_2 experiment at 2099 in RCP8.5) **(c)**, and indirect CO_2 effect on SOC (CO_2 experiment–fixed CO_2 experiment at 2099 in RCP8.5) in HadGEM. In **(a)**, the line of HWSD (broken black line) indicates the data from harmonized soil database (Hiederer and Köchy, 2011).

that the sensitivity of global SOC to ΔT varied among the biome models and that the present-day global SOC stock can be used to make more reliable SOC projections. Although actual global SOC stock estimation still has significant uncertainty, global SOC stock constraints are essential for reducing uncertainty in global SOC projections in ecosystem models.

Our simplified global dynamic model for the global SOC stock revealed that the balance of the global SOC stock turnover and input from VegC is quite different among the biome models, which further implies the different sensitivities to ΔT of the global SOC stocks among the biome models (Table 1). Hybrid4-simulated global SOC stocks decrease by 2099 in all RCPs because of the relatively high ΔT sensitivity in addition to the low turnover rate (high residence time) in VegC to SOC (Table 2, Friend et al., 2014). Although temperature is the most significant regulation factor of SOC dynamics (Raich and Schlesinger, 1992), discussion of the effect of increasing global mean temperature on SOC stocks is still lacking. According to our statistical analysis (Table 2), most biome models had adequate resolution to describe the global SOC stock change among the $\Delta 1\,^{\circ}C$ (or $2\,^{\circ}C$ for SDGVM) difference in the projection period. In these models, the global mean temperature ΔT could be a measure of the robustness of global SOC stock projection. However, the global SOC in JeDi was not sensitive to ΔT in this projection period. According to our estimation, the highest global SOC sensitivity was observed in VISIT, in which the rate of global SOC stock change was enhanced by $-6.95\,Pg\,C\,yr^{-1}$ in $\Delta\,4\,^{\circ}C$ (Fig. 3). However, the highest magnitude of SOC decomposition stimulated by increasing ΔT was observed in JULES ($-8.13\,Pg\,C\,yr^{-1}$ in $\Delta\,4\,^{\circ}C$) due to high global SOC stock in JULES. The Carnegie–Ames–Stanford approach model showed global SOC decomposition sensitivity of $2.26\,Pg\,C\,yr^{-1}\,\Delta\,^{\circ}C^{-1}$, which is nearly equivalent to results obtained from JULES when the $\Delta\,4\,^{\circ}C$ value was derived from simple extrapolation (Zhou et al., 2009). There is still a lack of observation-based estimation of global SOC response intensity to ΔT. Both global SOC stocks and data-oriented parameters such in Raich et al. (2002) could represent important information for the constraint and validation of global SOC dynamics.

However, β_2 was not effective for global SOC dynamics in all ecosystem models in our analysis, which does not mean

that precipitation is not important in SOC dynamics. Precipitation trends are globally heterogeneous; therefore, the representative ΔP might not be a useful index of SOC stock dynamics at a global scale in this projection period. However, precipitation is quite important in both soil decomposition (Falloon et al., 2011) and vegetation processes (Seneviratne et al., 2006), which considerably contribute to regional SOC dynamics.

4.2 SOC stock changes from vegetation dynamics and regional aspect

There were consistent latitudinal (geographic) patterns among the biome models (Figs. 5a, 1), and the highest SOC stock was observed between 40 and 75° N. However, we found that the amount of SOC stocks among the biome models significantly vary in this region. The models' SOC densities are different, possibly because of the balance of input and decomposition and the consideration of depth in the biome models (1 to 3 m or not explicit, Table 1). Tarnocai et al. (2009) estimated SOC stock depth up to 3 m, with a value of 1672 Pg C in permafrost-affected regions only. Thus, the SOC stock of this region and the global SOC stock in the biome models may be significantly underestimated.

From a regional perspective, the biome models showed quite different spatial patterns of SOC changes under HadGEM RCP8.5 (Figs. 4, 5), while the spatial patterns of VegC changes were generally more consistent among the biome models (Friend et al., 2014). We found that this spatial heterogeneity among the biome models was also present in the SOC stock changes in different scenarios (data not shown). In particular, in boreal to arctic regions, SOC acts as a sink and source of C depending on the biome model (Fig. 5). This result indicates that there is an underlying mechanistic difference among the biome models in these regions. Two models show decreased SOC stocks by 2099 in this region in HadGEM RCP8.5. LPJmL shows unique features in SOC stocks and changes in this region. This implies that high SOC accumulations (over 80 kg-C m^{-2}) (Figs. 5 and S1 in the Supplement) will be reduced with decreasing VegC by 2099 (Fig. S2 in the Supplement) in this region. This trend would result in low water availability in the permafrost regions, because the prediction is based on a mechanistic permafrost scheme (Beer et al., 2007; Schaphoff et al., 2013). Because LPJmL incorporated a freeze-and-thaw thermodynamics explicitly in discrete layers, it can simulate vertical water and carbon distributions in the model. This scheme enables LPJmL to describe the surface soil water deficit due to permafrost melting. Whereas, in Hybrid4, SOC decomposition is the main factor contributing to reduced SOC in this region. Dynamic vegetation and freeze–thaw schemes are important for SOC dynamics in permafrost zones, because they provide more accurate prediction of the balance of C input from successive vegetation and old soil carbon decomposition (Schuur et al., 2008, 2009; Schaphoff et al., 2013). However, in this study, dynamic vegetation and freeze–thaw schemes are only implemented in LPJmL. The potential release from SOC in permafrost regions could have a large impact on the global C cycle (Koven et al., 2011; Burke et al., 2012; MacDougall et al., 2012), and further model development is essential for the modification of projections for this region.

Previous extensive field research has shown that the CO_2 fertilizer effect on plant growth in higher CO_2 concentrations could also result in the accumulation of SOC (De Graaff et al., 2006). For the RCP8.5 climate forcing, the fixed CO_2 experiment suggested that the CO_2 fertilizer effect on plant production contributed considerably to the global SOC stock increase in all biome models. The indirect CO_2 fertilizer effect on the global SOC stock varied from 93 (Hybrid4) to 264 Pg C (VISIT) (mean $\pm$ SD; 196 ± 60 Pg C) at the end of the simulation period, while VegC stock increased from 295 to 645 Pg C (275 ± 150 Pg C) by 2099 because of increasing CO_2 (Figs. 2 and S2 in the Supplement). Thus, the CO_2 fertilizer effect on global SOC accumulation strongly affects the biome models, and further quantitative assessment might be needed. For example, Friend et al. (2014) focused their attention on the effects of CO_2 fertilizers on biomass production and turnover rate of biomass. In addition to the indirect CO_2 effects, other nutrient limitations (e.g., nitrogen and phosphorus) and their sensitivities could be large sources of uncertainty in SOC projection via vegetation production (Goll et al., 2012; Exbrayat et al., 2013). In our study framework, we cannot adequately validate these issues since only a few models consider them in their current versions (e.g., Hybrid4). Therefore, further interactions must be validated to more comprehensively understand the uncertainty sources in SOC projection.

A large variance in $\Delta SOC_{CO_2-\text{fixed}\,CO_2}/\Delta VegC_{CO_2-\text{fixed}\,CO_2}$ was observed among the biome models (Fig. 5d), suggesting that the vegetation–soil interactions including the vegetation turnover rate (Friend et al., 2014) and litter decomposition rate also had large uncertainties. This variance might cause an SOC projection difference among the biome models. To reduce these uncertainties, a more observation-based validation is desirable. For the litter decomposition process, for example, global database of the long-term intersite decomposition experiment team (LIDET) is one useful validation case study (Bonan et al., 2013). In addition, the process in SOC formation from alteration of litter via decomposition process (i.e., humification) and in their stabilization have not yet been implemented robustly in biome models when compared with actual SOC formation processes (Sollins et al., 1996; Six et al., 2002). This is another major process missing from the vegetation–soil interaction in biome models. To comprehensively address the biome model uncertainties in each successive process, the traceability framework developed by Xia et al. (2013) could be helpful.

4.3 SOC modeling issues

The accurate estimation of the present-day global SOC stock remains difficult because of a lack of appropriate broad and non-destructive investigation techniques to measure SOC stock, such as satellite-based remote sensing. In fact, current SOC was formed in slow turnover fractions over thousands of years (Trumbore, 2000). Therefore, when getting an initial SOC by the spin-up phase in biome models, there may not be enough information on the historical climate conditions and vegetation dynamics to duplicate in the entire SOC formation history. This is potentially one of the biggest issues for accurate estimation of SOC stock in biome models. In addition, observations of global long-term SOC stock dynamics for model validation are limited. Thus, it is very difficult to assess projected global SOC trends in each biome model. Therefore, in addition to quantitatively understanding the SOC stock, deductive inferences based on the extensive understanding of the processes are essential for minimizing uncertainties in SOC stock prediction. For example, the apparent variability in global SOC sensitivity to ΔT may result from differences in model structures and parameters. Regarding temperature sensitivity and the magnitude of response to rising temperatures, the following topics require improvement: (i) SOC compartments and their turnover rates (Jones et al., 2005; Conant et al., 2011), (ii) the temperature sensitivity parameter (e.g., Q_{10}) (Davidson and Janssens, 2006; Allison et al., 2010), and (iii) soil temperature prediction (radiation, heat production by microbes) (Luke and Cox, 2011; Khvorostyanov et al., 2008). In addition, microbial dynamics are a key component for the temperature acclimation of SOC decomposition (Todd-Brown et al., 2012; Wang et al., 2013). The acclimation response of SOC decomposition by microbial physiology is not included in the biome models used in this study. For SOC accumulation, soil mineralogical properties control soil C turnover (Torn et al., 1997). However, the biome models do not exploit global soil classification information (i.e., volcanic or non-volcanic soils), which still has significant uncertainties (Guillod et al., 2012; Hiederer and Köchy, 2011). In this study, peat and wetland soils are not explicitly simulated because of the large simulation grid size. Because of large carbon stock and water regime changes in future climates in such ecosystems, the SOC and soil-water-holding capacity feedback should also be considered in the SOC process in biome models (Ise et al., 2008). The interactions between SOC decomposition and nutrients (nitrogen) are also influential factors for global SOC projection (Manzoni and Porporato, 2007).

However, the details of these processes are beyond the scope of this study; therefore, we did not explore these issues in depth. A more specific model intercomparison, such as an environmental-response-function-based assessment (e.g., Falloon et al., 2011; Sierra et al., 2012; Exbrayat et al., 2013) is recommended. Furthermore, land-use change is not included in our projection; however, the effect of land-use changes on SOC dynamics is critical (Eglin et al., 2010). Estimating land-use change with high confidence is essential for accurate global SOC stock projections and could be used as a basis for policies that moderate the impacts of climate change.

5 Conclusions

The uncertainties associated with SOC projections are significantly high. The projected global SOC stocks by 2099 act as CO_2 sources or sinks depending on the biome model, even though models have similarly simulated historical SOC trends. The uncertainties of the SOC changes increase with higher forcing scenarios, and the global SOC stock change varies from -157 to 225 Pg C in HadGEM under RCP8.5 across biome models.

By adopting the simplified approach of global SOC as one compartment in the Earth system we can understand the comprehensive characteristics of each biome model on a global scale. The magnitude of SOC responses to global mean temperature increase considerably differed depending on the biome model. Our results confirmed that the SOC process implementations are dissimilar among the biome models at the global scale. In addition, global precipitation anomalies could not explain the simulated future global SOC stock changes. Moreover, the indirect CO_2 fertilizer effect contributed strongly to global SOC stock changes and projection uncertainties. For more reliable projections, both SOC dynamics and vegetation processes require reliable global SOC stock estimation and region-based improvements.

Supplementary material related to this article is available online at http://www.earth-syst-dynam.net/5/197/2014/esd-5-197-2014-supplement.pdf.

Acknowledgements. The authors wish to thank the ISI-MIP coordination team from the Potsdam Institute for Climate Impact Research. We acknowledge the World Climate Research Programme's Working Group on Coupled Modelling, which is responsible for CMIP. We also thank the climate modeling groups for producing and making their model output available. This study has been conducted under the ISI-MIP framework. The ISI-MIP Fast Track project was funded by the German Federal Ministry of Education and Research, project funding reference number 01LS1201A. Responsibility for the content of this publication lies with the authors. We also thank Naota Hanasaki and Yoshimitsu Masaki from the NIES for supporting the preparation of ISI-MIP settings. The research leading to these results has received funding from the European Community's Seventh Framework Programme (FP7 2007-2013) under grant agreement no. 238366. We appreciate the valuable comments from Seita Emori (NIES), Yoshiki Yamagata (NIES), and Rota Wagai (NIAES). This study was supported in part by the Environment Research and Technology Development Fund (S-10) of the Ministry of the Environment,

Japan. This study was also supported by the MEXT KAKENHI (no. 21114010). We also appreciate the editors, 3 reviewers, and Jeff Exbrayat (CCRC) for fundamental improvement of this manuscript.

Edited by: D. Lapola

References

Allison, S. D., Wallenstein, M. D., and Bradford, M. A.: Soil-carbon response to warming dependent on microbial physiology, Nat. Geosci., 3, 336–340, 2010.

Batjes, N.: Total carbon and nitrogen in the soils of the world, European J. Soil Sci., 47, 151–163, doi:10.1111/j.1365-2389.1996.tb01386.x, 1996.

Beer, C., Lucht, W., Gerten, D., Thonicke, K., and Schmullius, C.: Effects of soil freezing and thawing on vegetation carbon density in Siberia: A modeling analysis with the Lund-Potsdam-Jena Dynamic Global Vegetation Model (LPJ-DGVM), Global Biogeochem. Cy., 21, GB1012, doi:10.1029/2006GB002760, 2007.

Best, M. J., Pryor, M., Clark, D. B., Rooney, G. G., Essery, R .L. H., Ménard, C. B., Edwards, J. M., Hendry, M. A., Porson, A., Gedney, N., Mercado, L. M., Sitch, S., Blyth, E., Boucher, O., Cox, P. M., Grimmond, C. S. B., and Harding, R. J.: The Joint UK Land Environment Simulator (JULES), model description – Part 1: Energy and water fluxes, Geosci. Model Dev., 4, 677–699, doi:10.5194/gmd-4-677-2011, 2011.

Bohn, H. L.: Estimate of organic carbon in world soils, Soil Sci. Soc. Am. J., 40, 468–470, 1976.

Bolin, B.: The carbon cycle, Scient. Am., 223, 125–132, 1970.

Bonan, G. B., Hartman, M. D., Parton, W. J., and Wieder, W. R.: Evaluating litter decomposition in earth system models with long-term litterbag experiments: an example using the Community Land Model version 4 (CLM4), Global Change Biol., 19, 957–974, 2013.

Breure, A., De Deyn, G., Dominati, E., Eglin, T., Hedlund, K., Van Orshoven, J., and Posthuma, L.: Ecosystem services: a useful concept for soil policy making!, Curr. Opin. Environ. Sus., 4, 578–585, 2012.

Burke, E. J., Hartley, I. P., and Jones, C. D.: Uncertainties in the global temperature change caused by carbon release from permafrost thawing, The Cryosphere, 6, 1063–1076, doi:10.5194/tc-6-1063-2012, 2012.

Clark, D. B., Mercado, L. M., Sitch, S., Jones, C. D., Gedney, N., Best, M. J., Pryor, M., Rooney, G. G., Essery, R. L. H., Blyth, E., Boucher, O., Harding, R. J., Huntingford, C., and Cox, P. M.: The Joint UK Land Environment Simulator (JULES), model description – Part 2: Carbon fluxes and vegetation dynamics, Geosci. Model Dev., 4, 701–722, doi:10.5194/gmd-4-701-2011, 2011.

Conant, R., Ryan, M., Ågren, G., Birge, H., Davidson, E., Eliasson, P., Evans, S., Frey, S., Giardina, C., Hopkins, F., Hyvönen, R., Kirschbaum, M. U. F., Lavallee, J. M., Leifeld, J., Parton, W. J., Megan Steinweg, J., Wallenstein, M. D., Martin Wetterstedt, J. Å., and Bradford, M. A.: Temperature and soil organic matter decomposition rates–synthesis of current knowledge and a way forward, Global Change Biol., 17, 3392–3404, doi:10.1111/j.1365-2486.2011.02496.x, 2011.

Davidson, E. and Janssens, I.: Temperature sensitivity of soil carbon decomposition and feedbacks to climate change, Nature, 440, 165–173, 2006.

De Graaff, M. A., Van Groningen, K. J. A. N., Six, J., Hungate, B., and van Kessel, C.: Interactions between plant growth and soil nutrient cycling under elevated CO_2: A meta-analysis, Global Change Biol., 12, 2077–2091, 2006.

Eglin, T., Ciais, P., Piao, S., Barre, P., Bellassen, V., Cadule, P., Chenu, C., Gasser, T., Koven, C., Reichstein, M., and Smith, P.: Historical and future perspectives of global soil carbon response to climate and land-use changes, Tellus B, 62, 700–718, 2010.

Exbrayat, J.-F., Pitman, A. J., Zhang, Q., Abramowitz, G., and Wang, Y.-P.: Examining soil carbon uncertainty in a global model: response of microbial decomposition to temperature, moisture and nutrient limitation, Biogeosciences, 10, 7095–7108, doi:10.5194/bg-10-7095-2013, 2013.

Falloon, P., Jones, C., Ades, M., and Paul, K.: Direct soil moisture controls of future global soil carbon changes: An important source of uncertainty, Global Biogeochem. Cy., 25, GB3010, doi:10.1029/2010GB003938, 2011.

Friedlingstein, P., Cox, P., Betts, R., Bopp, L., Von Bloh, W., Brovkin, V., Cadule, P., Doney, S., Eby, M., Fung, I., Bala, G., John, J., Jones, C., Joos, F., Kato, T., Kawamiya, M., Knorr, W., Lindsay, K., Matthews, H. D., Raddatz, T., Rayner, P., Reick, C., Roeckner, E., Schnitzler, K. G., Schnur, R., Strassmann, K., Weaver, A. J., Yoshikawa, C., and Zeng, N.: Climate-carbon cycle feedback analysis: Results from the C4MIP model intercomparison, J. Climate, 19, 3337–3353, 2006.

Friend, A. D. and White, A.: Evaluation and analysis of a dynamic terrestrial ecosystem model under preindustrial conditions at the global scale, Global Biogeochem. Cy., 14, 1173–1190, 2000.

Friend, A. D., Betts, R., Cadule, P., Ciais, P., Clerk, D., Dankers, R., Falloon, P., Gerten, D., Itoh, A., Kahana, R., Keribin, R. M., Kleidon, A., Lomas, M. R., Nishina, K., Ostberg, S., Pavlick, R., Peylin, P., Rademacher, T. T., Schaphoff, S., Vuichard, N., Wiltshire, A., and Woodward, F. I.: Anticipating terrestrial ecosystem response to future climate change and increase in atmospheric CO_2, P. Natl. Acad. Sci. USA, 111, 3225–3227, 2014.

Goll, D. S., Brovkin, V., Parida, B. R., Reick, C. H., Kattge, J., Reich, P. B., van Bodegom, P. M., and Niinemets, Ü.: Nutrient limitation reduces land carbon uptake in simulations with a model of combined carbon, nitrogen and phosphorus cycling, Biogeosciences, 9, 3547–3569, doi:10.5194/bg-9-3547-2012, 2012.

Guillod, B., Davin, E., Kündig, C., Smiatek, G., and Seneviratne, S.: Impact of soil map specifications for European climate simulations, Clim. Dynam., 40, 1–19, 2012.

Heimann, M. and Reichstein, M.: Terrestrial ecosystem carbon dynamics and climate feedbacks, Nature, 451, 289–292, 2008.

Hempel, S., Frieler, K., Warszawski, L., Schewe, J., and Piontek, F.: A trend-preserving bias correction – the ISI-MIP approach, Earth Syst. Dynam., 4, 219–236, doi:10.5194/esd-4-219-2013, 2013.

Hiederer, R. and Köchy, M.: Global soil organic carbon estimates and the harmonized world soil database, EUR 25225EN, Publ. Off. of the Eur. Union, Luxembourg, 2011.

Ise, T. and Moorcroft, P.: The global-scale temperature and moisture dependencies of soil organic carbon decomposition: an analysis using a mechanistic decomposition model, Biogeochemistry, 80, 217–231, 2006.

Ise, T., Dunn, A., Wofsy, S., and Moorcroft, P.: High sensitivity of peat decomposition to climate change through water-table feedback, Nat. Geosci., 1, 763–766, 2008.

Ito, A. and Inatomi, M.: Water-use efficiency of the terrestrial biosphere: a model analysis focusing on interactions between the global carbon and water cycles, J. Hydrometeorol., 13, 681–694, 2012.

Ito, A. and Oikawa, T.: A simulation model of the carbon cycle in land ecosystems (Sim-CYCLE): a description based on dry-matter production theory and plot-scale validation, Ecol. Model., 151, 143–176, 2002.

Jones, C., McConnell, C., Coleman, K., Cox, P., Falloon, P., Jenkinson, D., and Powlson, D.: Global climate change and soil carbon stocks; predictions from two contrasting models for the turnover of organic carbon in soil, Global Change Biol., 11, 154–166, 2005.

Khvorostyanov, D., Krinner, G., Ciais, P., Heimann, M., and Zimov, S.: Vulnerability of permafrost carbon to global warming, Part I: model description and role of heat generated by organic matter decomposition, Tellus B, 60, 250–264, 2008.

Koven, C., Ringeval, B., Friedlingstein, P., Ciais, P., Cadule, P., Khvorostyanov, D., Krinner, G., and Tarnocai, C.: Permafrost carbon-climate feedbacks accelerate global warming, P. Natl. Acad. Sci. USA, 108, 14769–14774, 2011.

Krinner, G., Viovy, N., de Noblet-Ducoudré, N., Ogée, J., Polcher, J., Friedlingstein, P., Ciais, P., Sitch, S., and Prentice, I.: A dynamic global vegetation model for studies of the coupled atmosphere-biosphere system, Global Biogeochem. Cy., 19, GB1015, doi:10.1029/2003GB002199, 2005.

Lal, R.: Soil carbon sequestration impacts on global climate change and food security, Science, 304, 1623–1627, 2004.

Lal, R.: Beyond Copenhagen: mitigating climate change and achieving food security through soil carbon sequestration, Food Secur., 2, 169–177, 2010.

Li, J., Wang, G., Allison, S., Mayes, M., and Luo, Y.: Soil carbon sensitivity to temperature and carbon use efficiency compared across microbial-ecosystem models of varying complexity, Biogeochemistry, doi:10.1007/s10533-013-9948-8, in press, 2014.

Luke, C. and Cox, P.: Soil carbon and climate change: from the Jenkinson effect to the compost-bomb instability, Eur. J. Soil Sci., 62, 5–12, 2011.

MacDougall, A., Avis, C., and Weaver, A.: Significant contribution to climate warming from the permafrost carbon feedback, Nat. Geosci., 5, 719–721, doi:10.1038/ngeo1573, 2012.

Manzoni, S. and Porporato, A.: A theoretical analysis of nonlinearities and feedbacks in soil carbon and nitrogen cycles, Soil Biol. Biochem., 39, 1542–1556, 2007.

Mol, G. and Keesstra, S.: Soil science in a changing world, Curr. Opin. Environ. Sus., 4, 473–477, doi:10.1016/j.cosust.2012.10.013, 2012.

Pavlick, R., Drewry, D. T., Bohn, K., Reu, B., and Kleidon, A.: The Jena Diversity-Dynamic Global Vegetation Model (JeDi-DGVM): a diverse approach to representing terrestrial biogeography and biogeochemistry based on plant functional trade-offs, Biogeosciences, 10, 4137–4177, doi:10.5194/bg-10-4137-2013, 2013.

Post, W., Emanuel, W., Zinke, P., and Stangenberger, A.: Soil carbon pools and world life zones, Nature, 298, 156–159, 1982.

Raichi, J. W. and Schlesinger, W.: The global carbon dioxide flux in soil respiration and its relationship to vegetation and climate, Tellus B, 44, 81–99, 1992.

Raichi, J. W., Potter, C. S., and Bhagawati, D.: Interannual variability in global soil respiration, 1980–94, Global Change Biol., 8, 800–812, 2002.

R Core Team: R: A Language and Environment for Statistical Computing, available at: http://www.R-project.org/, R Foundation for Statistical Computing, Vienna, Austria,2012.

Ruesch, A. and Gibbs, H. K.: New IPCC Tier-1 global biomass carbon map for the year 2000, Carbon Dioxide Information Analysis Center (CDIAC), available at: http://cdiac.ornl.gov, Oak Ridge National Laboratory, Oak Ridge, Tennessee, 2008.

Schaphoff, S., Heyder, U., Ostberg, S., Gerten, D., Heinke, J., and Lucht, W.: Contribution of permafrost soils to the global carbon budget, Environ. Res. Lett., 8, 014026, doi:10.1088/1748-9326/8/1/014026, 2013.

Schuur, E., Bockheim, J., Canadell, J., Euskirchen, E., Field, C., Goryachkin, S., Hagemann, S., Kuhry, P., Lafleur, P., Lee, H., Mazhitova, G., Nelson, F. E., Rinke, A., Romanovsky, V. E., Shiklomanov, N., Tarnocai, C., Venevsky, S., Vogel, J. G., and Zimov, S. A.: Vulnerability of permafrost carbon to climate change: Implications for the global carbon cycle, Bioscience, 58, 701–714, 2008.

Schuur, E., Vogel, J., Crummer, K., Lee, H., Sickman, J., and Osterkamp, T.: The effect of permafrost thaw on old carbon release and net carbon exchange from tundra, Nature, 459, 556–559, 2009.

Seneviratne, S., Lüthi, D., Litschi, M., and Schär, C.: Land–atmosphere coupling and climate change in Europe, Nature, 443, 205–209, 2006.

Sierra, C. A., Müller, M., and Trumbore, S. E.: Models of soil organic matter decomposition: the SoilR package, version 1.0, Geosci. Model Dev., 5, 1045-1060, doi:10.5194/gmd-5-1045-2012, 2012.

Sims, C. and Zha, T.: Bayesian methods for dynamic multivariate models, Int. Econ. Rev., 39, 949–968, 1998.

Sitch, S., Smith, B., Prentice, I., Arneth, A., Bondeau, A., Cramer, W., Kaplan, J., Levis, S., Lucht, W., Sykes, M., Thonicke, K., and Venevsky, S.: Evaluation of ecosystem dynamics, plant geography and terrestrial carbon cycling in the LPJ dynamic global vegetation model, Global Change Biol., 9, 161–185, 2003.

Sitch, S., Huntingford, C., Gedney, N., Levy, P., Lomas, M., Piao, S., Betts, R., Ciais, P., Cox, P., Friedlingstein, P., Jones, C. D., Prentice, I. C., and Woodward, F. I.: Evaluation of the terrestrial carbon cycle, future plant geography and climate-carbon cycle feedbacks using five Dynamic Global Vegetation Models (DGVMs), Global Change Biol., 14, 2015–2039, 2008.

Six, J., Conant, R., Paul, E., and Paustian, K.: Stabilization mechanisms of soil organic matter: implications for C-saturation of soils, Plant Soil, 241, 155–176, 2002.

Sollins, P., Homann, P., and Caldwell, B. A.: Stabilization and destabilization of soil organic matter: mechanisms and controls, Geoderma, 74, 65–105, 1996.

Stan Development Team: Stan: A C++ Library for Probability and Sampling, Version 1.0, available at: http://mc-stan.org/ (last access: January 2013), 2012.

Tarnocai, C., Canadell, J., Schuur, E., Kuhry, P., Mazhitova, G., and Zimov, S.: Soil organic carbon pools in the northern circumpolar permafrost region, Global Biogeochem. Cy., 23, GB2023, doi:10.1029/2008GB003327, 2009.

Thum, T., Räisänen, P., Sevanto, S., Tuomi, M., Reick, C., Vesala, T., Raddatz, T., Aalto, T., Järvinen, H., Altimir, N., Pilegaard, K., Nagy, Z., Rambal, S., and Liski, J.: Soil carbon model alternatives for ECHAM5/JSBACH climate model: Evaluation and impacts on global carbon cycle estimates, J. Geophys. Res., 116, G02028, doi:10.1029/2010JG001612, 2011.

Todd-Brown, K. E. O., Hopkins, F., Kivlin, S., Talbot, J., and Allison, S.: A framework for representing microbial decomposition in coupled climate models, Biogeochemistry, 109, 19–33, 2012.

Todd-Brown, K. E. O., Randerson, J. T., Post, W. M., Hoffman, F. M., Tarnocai, C., Schuur, E. A. G., and Allison, S. D.: Causes of variation in soil carbon simulations from CMIP5 Earth system models and comparison with observations, Biogeosciences, 10, 1717–1736, doi:10.5194/bg-10-1717-2013, 2013.

Torn, M., Trumbore, S., Chadwick, O., Vitousek, P., and Hendricks, D.: Mineral control of soil organic carbon storage and turnover, Nature, 389, 170–173, 1997.

Trumbore, S.: Age of soil organic matter and soil respiration: radiocarbon constraints on belowground C dynamics, Ecol. Appl., 10, 399–411, 2000.

Wang, G., Post, W., and Mayes, M.: Development of microbial-enzyme-mediated decomposition model parameters through steady-state and dynamic analyses, Ecol. Appl., 23, 255–272, doi:10.1890/12-0681.1, 2013.

Warszawski, L., Frieler, K., Huber, V., Piontek, F., Serdeczny, O., and Schewe, J.: The Inter-Sectoral Impact Model Intercomparison Project (ISI-MIP): Project framework., P. Natl. Acad. Sci. USA, 111, 3228–3232, 2014.

Wershaw, R.: Model for humus in soils and sediments, Environ. Sci. Technol., 27, 814–816, 1993.

Woodward, F., Smith, T., and Emanuel, W.: A global land primary productivity and phytogeography model, Global Biogeochem. Cy., 9, 471–490, 1995.

Xia, J., Luo, Y., Wang, Y.-P., and Hararuk, O.: Traceable components of terrestrial carbon storage capacity in biogeochemical models, Global Change Biol., 2013.

Zhou, T., Shi, P., Hui, D., and Luo, Y.: Global pattern of temperature sensitivity of soil heterotrophic respiration (Q_{10}) and its implications for carbon-climate feedback, J. Geophys. Res.-Biogeo., 114, G02016, doi:10.1029/2008JG000850, 2009.